

TWO-SOURCE ENERGY BALANCE MODEL: REFINEMENTS AND LYSIMETER TESTS IN THE SOUTHERN HIGH PLAINS



P. D. Colaizzi, S. R. Evett, T. A. Howell, P. H. Gowda,
S. A. O'Shaughnessy, J. A. Tolck, W. P. Kustas, M. C. Anderson

ABSTRACT. A thermal two-source energy balance model (TSEB-N95) was evaluated for calculating daily evapotranspiration (ET) of corn, cotton, grain sorghum, and wheat in a semiarid, advective environment. Crop ET was measured with large, monolithic weighing lysimeters. The TSEB-N95 model solved the energy budget of soil and vegetation using a series resistance network, and one-time-of-day latent heat flux calculations were scaled to daily ET using the ASCE Standardized Reference ET equation for a short crop. The TSEB-N95 model included several refinements, including a geometric method to account for the nonrandom spatial distribution of vegetation for row crops with partial canopy cover, where crop rows were modeled as elliptical hedgerows. This geometric approach was compared to the more commonly used, semi-empirical clumping index approach. Both approaches resulted in similar ET calculations, but the elliptical hedgerow approach performed slightly better. Using the clumping index, root mean squared error, mean absolute error, and mean bias error were 1.0 (22%), 0.79 (17%), and 0.093 (2.0%) mm d^{-1} , respectively, between measured and calculated daily ET for all crops, where percentages were of the measured mean ET (4.62 mm d^{-1}). Using the elliptical hedgerow, root mean squared error, mean absolute error, and mean bias error were 0.86 (19%), 0.69 (15%), and 0.17 (3.6%) mm d^{-1} , respectively, between measured and calculated daily ET for all crops. The refinements to TSEB-N95 will improve the accuracy of remote sensing-based ET maps, which is imperative for water resource management.

Keywords. Clumping index, Evapotranspiration, Fractional cover, Latent heat flux, Radiometric temperature, Remote sensing, Row crops, Texas.

Judicious irrigation management is expected to play a key role in mitigating the dilemma of increased demands for agricultural production by an expanding world population and rapidly declining available water resources. Irrigation management entails numerous strategies, such as time- and site-specific water application, deficit or limited irrigation, and various combinations of these. Implementing these strategies has been impeded by

the lack of automated, real-time information on crop and soil water conditions, such as maps of crop evapotranspiration (ET) and crop water stress. Consequently, adoption of advanced irrigation management techniques has lagged compared with other industrial systems, where feedback, automation, and decision support systems are more routinely used (Evans and King, 2010). As irrigated farms continue to consolidate (USDA-NASS, 2008), it is expected that larger areas will be managed by fewer personnel. Therefore, feedback and information systems tailored to reduce management time will be essential to maintain farm profitability with decreasing available water.

Remote sensing, in which the reflectance and temperature of the surface is measured by non-contact radiometers, was recognized as a potential feedback tool for agricultural management at least since the 1960s (e.g., Park et al., 1968). Several remote sensing algorithms are available to calculate ET and quantify crop water stress. The thermal-based algorithms typically combine reflectance and thermal measurements of a vegetated surface with point-based agricultural meteorological data to drive a surface energy balance model, in which the remotely sensed and meteorological data provide the spatial and temporal domains, respectively. Since remotely sensed surface temperature is often a composite of vegetation and soil temperatures, especially for row crops, two-source energy balance (TSEB) models have become popular. These mod-

Submitted for review in August 2011 as manuscript number SW 9315; approved for publication by the Soil & Water Division of ASABE in March 2012. Presented at the 5th National Decennial Irrigation Conference as Paper No. IRR109701.

The use of trade, firm, or corporation names in this article is for the information and convenience of the reader. Such use does not constitute an official endorsement or approval by the USDA of any product or service to the exclusion of others that may be suitable. The USDA is an equal opportunity provided and employer.

The authors are **Paul D. Colaizzi**, ASABE Member, Research Agricultural Engineer, **Steven R. Evett**, ASABE Member, Research Soil Scientist, **Terry A. Howell**, ASABE Fellow, Laboratory Director and Research Leader, **Prasanna H. Gowda**, ASABE Member, Research Agricultural Engineer, **Susan A. O'Shaughnessy**, ASABE Member, Research Agricultural Engineer, and **Judy A. Tolck**, Research Plant Physiologist, USDA-ARS Conservation and Production Research Laboratory, Bushland, Texas; and **William P. Kustas**, Hydrologist, and **Martha C. Anderson**, Research Physical Scientist, USDA-ARS Hydrology and Remote Sensing Laboratory, Beltsville Maryland. **Corresponding author:** Paul D. Colaizzi, USDA-ARS, P.O. Drawer 10, 2300 Experiment Station Rd., Bushland, Texas 79012-0010; phone: 806-356-5763; e-mail: Paul.Colaizzi@ars.usda.gov.

els solve the energy balance of the soil and canopy sources separately and combine these to derive the total latent heat flux of the surface. Norman et al. (1995) developed an operational TSEB model (hereafter designated TSEB-N95) that only required input data and parameters that were either readily available or could be reasonably calculated based on knowledge of local vegetation and soil characteristics. Kustas and Norman (1999, 2000) described several refinements to TSEB-N95, including use of the Campbell and Norman (1998) radiation scattering model, estimation of soil resistance to heat transport, and the effects of the nonrandom spatial distribution of vegetation. Nonrandom spatial distribution of vegetation commonly occurs for row crops or sparse heterogeneous natural vegetation and results in different partitioning of energy fluxes to the soil and canopy compared with a uniform, homogenous canopy. Nonrandom spatial distribution of vegetation has been commonly accounted for by using the clumping index approach (e.g., Chen and Cihlar, 1995), which is a semi-empirical factor that is multiplied by the leaf area index and has been adopted for row crops (e.g., Kustas and Norman, 1999; Anderson et al., 2005). The clumping index has different values for solar beam irradiance, diffuse irradiance, and the view factor of a directional radiometer. In the row crop formulation, the clumping index depends on the zenith and azimuth view angles relative to the rows, row spacing, and canopy height and width.

Numerous studies have tested TSEB-N95 for a variety of locations, climates, and vegetation types. A few examples include grass and desert shrubs near Tombstone, Arizona (Norman et al., 1995); prairie grass near Manhattan, Kansas (Norman et al., 1995); irrigated cotton near Maricopa, Arizona (Kustas, 1990; Kustas and Norman, 1999, 2000); rangeland, pasture, and bare soil near El Reno, Oklahoma (Norman et al., 2000); a riparian zone along the Rio Grande in the Bosque Del Apache National Wildlife Refuge in central New Mexico (Norman et al., 2000); corn, soybean, and bare soil near Ames, Iowa (Li et al., 2005; Anderson et al., 2005); and irrigated spring wheat near Maricopa, Arizona (French et al., 2007). Nearly all of these studies used Bowen ratio, eddy covariance, or meteorological-flux tower (METFLUX) techniques for ground truth measurements of energy fluxes, although French et al. (2007) derived ET from a soil water balance using neutron probe measurements. These systems are relatively portable, low cost, and robust. However, the Bowen ratio method assumes that fluxes are vertical and is therefore subject to errors during advective conditions and can also be sensitive to fetch and instrument bias (Todd et al., 2000). Eddy covariance techniques measure turbulent fluxes across a field, but the energy balance is often not closed (Twine et al., 2000) even if additional procedures or corrections are used (e.g., Chavez et al., 2009). Few, if any, studies have tested TSEB-N95 using weighing lysimeters, which can be the most accurate means of measuring ET (Howell et al., 1995a, 1997). The USDA-ARS Conservation and Production Research Laboratory at Bushland, Texas, has measured ET using large, monolithic weighing lysimeters for several major crops in the U.S. Southern High Plains. This region is semi-arid and is characterized by very high atmospheric

demand due to strong regional advection, abundant solar irradiance, and high vapor pressure deficits. It therefore represents a unique location for studies in energy balance and ET models.

Preliminary tests of TSEB-N95 (which included refinements described by Kustas and Norman, 1999) were conducted at Bushland for several row crops, where ET was measured by weighing lysimeters and surface temperature was measured by stationary infrared thermometers (IRTs) viewing the lysimeter surface. Large errors were observed for partial canopy cover, and large errors were also obtained for partial canopy cover when comparing measurements of transmitted and reflected radiation with those calculated by the Campbell and Norman (1998) radiative transfer model. In both models, the widely used clumping index approach was used to account for the nonrandom spatial distribution of row crop vegetation. The clumping index formulations do not directly account for the circular or elliptical footprint of a ground-based radiometer, which would result in a different fraction of vegetation appearing in the footprint compared with a square pixel (i.e., obtained from satellite or airborne scanners). In addition, the clumping index does not directly account for the different portions of sunlit and shaded soil, which depend on solar zenith and azimuth angle relative to row orientation and have a large impact on radiation partitioning to the soil and canopy and hence ET. Since many row crops under center-pivot irrigation are planted in a circle, row orientation would be expected to contribute to the spatial variability of ET, especially for partial canopy cover.

To address these limitations, Colaizzi et al. (2010) developed a method to calculate the fraction of soil and vegetation of a row crop appearing in a radiometer footprint, and Colaizzi et al. (2012a, 2012b) described and tested a modification to the Campbell and Norman (1998) radiative transfer model in accounting for the spatial distribution of row crop vegetation. These studies explicitly accounted for row crop geometry by modeling crop rows as elliptical hedgerows. The elliptical hedgerow approach consistently improved calculations of soil and vegetation appearing within the radiometer footprint, as well as calculations of transmitted and reflected radiation, compared with the clumping index approach. The objectives of this study were to test TSEB-N95 where the nonrandom spatial distribution of row crop vegetation was accounted for using the elliptical hedgerow approach, and compare these results with the clumping index approach.

MATERIALS AND METHODS

TWO-SOURCE MODEL OVERVIEW

Most energy balance algorithms, including TSEB-N95, consider the four major energy flux components of the soil-canopy-atmosphere continuum, which are net radiation (R_N), soil heat flux (G), sensible heat flux (H), and latent heat flux (LE), and assume that other energy components such as canopy heat storage and photosynthesis are negligible. The available energy is equal to the turbulent fluxes, expressed as $R_N - G = H + LE$, where turbulent fluxes are

positive away from the canopy. In TSEB-N95, R_N , H , and LE are further partitioned to their canopy and soil components, and the energy balance is expressed as:

$$LE_C = R_{N,C} - H_C \quad (1a)$$

$$LE_S = R_{N,S} - G - H_S \quad (1b)$$

where the subscripts C and S refer to the canopy and soil, respectively. $R_{N,C}$ and $R_{N,S}$ were determined by the canopy radiative transfer model of Campbell and Norman (1998), which calculates the photosynthetic, near-infrared, and longwave components separately. Non-homogeneous canopies, such as forests and row crops, scatter radiation differently than homogeneous canopies. Campbell and Norman (1998) suggested that this could be accounted for by multiplying leaf area index by a simple clumping index, which has been demonstrated operationally (e.g., Kustas and Norman, 1999; Anderson et al., 2005). However, Colaizzi et al. (2012a, 2012b) accounted for the nonrandom spatial distribution of row crop vegetation by modeling crop rows as elliptical hedgerows, which was also used to calculate $R_{N,S}$ and $R_{N,C}$.

Previous TSEB-N95 studies have usually calculated G as a constant fraction of $R_{N,S}$; however, G may exhibit a strong phase difference with $R_{N,S}$, which was observed at our location. Therefore, G was calculated using a phase difference equation described by Santanello and Friedl (2003):

$$G = R_{N,S} \left\{ a \cdot \cos \left[\frac{2\pi}{b} (t + c) \right] \right\} \quad (2)$$

where t is the solar time angle (s), and a , b , and c are empirical constants. Santanello and Friedl (2003) showed that these parameters depend on near-surface soil water content as well as other soil characteristics. In the present study, $a = 0.30$, $b = 80,000$ s, and $c = 3,600$ s were derived by maximizing the modified coefficient of model efficiency (Legates and McCabe, 1999) between G calculated by equation 2 and G calculated by measurements of soil heat flux and soil temperature and calculations of soil water content near the surface (Evet et al., 2012). Parameters a , b , and c were optimized with the Microsoft Excel Solver add-in feature (Excel SP3, Microsoft Corp., Redlands, Wash.), where parameters were constrained to physically plausible values ($0.10 \leq a \leq 0.50$; $72,000 \leq b \leq 86,400$; $0 \leq c \leq 14,400$) and precision was 0.01 for a and 100 s for b and c . A more exhaustive study on soil heat flux models is presently under-

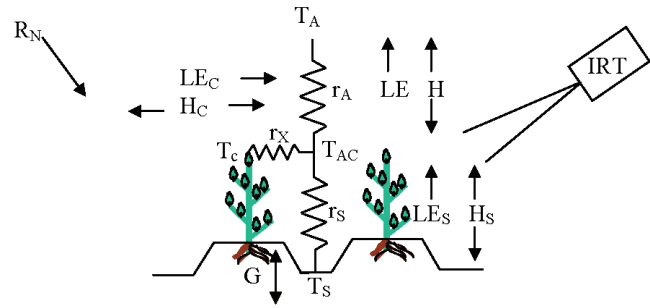


Figure 1. Series resistances and flux components for TSEB-N95 (adopted from Norman et al., 1995, fig. 11). See text for symbol definitions.

way using field measurements at our location (Evet et al., 2012).

H is calculated by temperature gradient-transport resistance networks between the soil, canopy, and air above. The networks were formulated as either parallel or series by Norman et al. (1995). In the parallel network, turbulent fluxes occur as separate (parallel) streams between the soil or canopy and atmosphere, and there is no direct interaction between the soil and canopy. In the series network, flux exchange between the soil and canopy may occur directly (fig. 1). Li et al. (2005) reported that the parallel model was more sensitive to errors in vegetation cover calculations, and that these uncertainties may be moderated by the additional parameter of within-canopy air temperature that is used in the series formulation (T_{AC} in fig. 1). Kustas and Norman (1999), Kustas et al. (2004), and Li et al. (2005) concluded that the series was preferable over the parallel model for heterogeneous landscapes containing a large range of vegetation cover. Since the present study included four different crops (table 1) having a wide range of vegetation cover, we used the series formulation.

The canopy, soil, and composite sensible heat flux components in figure 1 are expressed as:

$$H_C = \rho C_p \frac{T_C - T_{AC}}{r_X} \quad (3a)$$

$$H_S = \rho C_p \frac{T_S - T_{AC}}{r_S} \quad (3b)$$

$$H = \rho C_p \frac{T_{AC} - T_A}{r_A} \quad (3c)$$

where ρ is the air density (kg m^{-3}); C_p is the specific heat of

Table 1. Crops for which evapotranspiration was measured using monolithic weighing lysimeters, and the lower (T_{base}) and upper (T_{peak}) air temperature limits used to calculate growing degree days.

Crop	Season and Lysimeter ^[a]	Irrigation Rate (% ET replacement)	T_{base} (°C)	T_{peak} (°C)	Additional References
Corn	1989, NE and SE	100%	10.0	30.0	Howell et al. (1995a), Howell et al. (1997), Tolck et al. (1995)
Cotton	2008, NE and SE	100%	15.6	50.0	Howell et al. (2004), Evett et al. (2012)
Grain sorghum	1998, NW and SW	Dryland	10.0	37.8	
Winter wheat	1991-1992, NE and SE	100% (NE), 50% (SE)	0.0	26.1	Evet et al. (1994), Howell et al. (1995a), Howell et al. (1995b), Howell et al. (1997)

^[a] Each lysimeter is located in a field quadrant and is designated as NE = northeast, SE = southeast, NW = northwest, and SW = southwest.

air (assumed constant at $1013 \text{ kJ kg}^{-1} \text{ K}^{-1}$); T_C , T_A , T_S , and T_{AC} are the temperatures of the canopy, air, soil, and air temperature within the canopy boundary layer, respectively (K); r_X is the resistance in the boundary layer near the canopy (s m^{-1}); r_S is the resistance to heat flux in the boundary layer immediately above the soil surface (s m^{-1}); and r_A is the aerodynamic resistance (s m^{-1}). In equation 3c, $T_{AC} < T_A$ results in negative H , which may include advected energy. The directional radiometric surface temperature (T_R , derived from remotely sensed directional brightness temperature) was assumed related to T_C and T_S as:

$$T_R^4 = f_{VR} T_C^4 + (1 - f_{VR}) T_S^4 \quad (4)$$

where f_{VR} is the fraction of vegetation appearing in the radiometer field-of-view where directional brightness temperature is measured. In order to solve the temperature and resistance network, T_C is initially calculated using the Priestley-Taylor approximation for latent heat flux (Priestley and Taylor, 1972); the Priestley-Taylor parameter (α_{PT}) of 1.3 was used for the present study location (Agam et al., 2010). In equation 4, f_{VR} never physically reaches 1.0 because of canopy extinction, but this constraint would be required in any case in order to solve for T_S . If f_{VR} is close to 1.0, then T_S can be sensitive to small errors in f_{VR} , resulting in unrealistic values. Therefore, T_S was constrained from falling below the air wet bulb temperature, where the wet bulb temperature is the lower limit for an evaporating surface (Wanjura and Upchurch, 1996). In the case of water-stressed vegetation, non-transpiring canopy elements (e.g., senesced leaves or non-leaf elements), or low vapor pressure deficit, T_C may be under-calculated, resulting in over-calculations of T_S and H_S , and possibly resulting in $LE_S < 0$ (from eq. 1b). This would imply condensation at the soil surface, which is unlikely for conditions expected when obtaining remote sensing measurements (i.e., near midday and clear skies), especially in less humid climates. Therefore, if the model solution resulted in $LE_S < 0$, then α_{PT} was reduced below 1.3 in increments of 0.1 until $LE_S \geq 0$. For a dry soil surface, it is possible that the resulting LE_S could still be negative even though $\alpha_{PT} = 0$. In this case, LE_S is set to zero, and from equation 1b, $H_S = R_{N,S} - G$, and the remaining energy flux components are recalculated according to these constraints. The rationale for the Priestley-Taylor approximation and procedures for calculating the temperatures and resistances in equations 3 and 4 are provided by Norman et al. (1995) and Kustas and Norman (1999).

Irrigation management typically entails using a soil water balance to calculate soil water depletion at daily time steps, and this requires calculation of daily evapotranspiration (ET). Therefore, daily ET was derived from instantaneous total latent heat flux (i.e., $LE = LE_C + LE_S$) by first converting LE to ET at 30 min time steps and then using a one-time-of-day calculation of 30 min ET to calculate daily ET. LE was converted to 30 min ET averages by multiplying by 1800 s and dividing by the latent heat of vaporization (λ), where $\lambda = 2.501 - 0.002361 T_A$, and λ is in MJ kg^{-1} and T_A is air temperature in $^{\circ}\text{C}$, and assuming the density of water is constant at 1000 kg m^{-3} . Daytime λ was typically 2.44 MJ kg^{-1} at the study location. The 30 min ET average

during solar noon (12:30 to 13:00 at the study location) was scaled to daily ET as:

$$ET_{24} = ET_{0.5} \left(\frac{ET_{OS-24}}{ET_{OS-0.5}} \right) \quad (5)$$

where ET_{24} is the daily (24 h) calculated ET, $ET_{0.5}$ is the 30 min calculated ET (calculated from LE), $ET_{OS-0.5}$ is the ASCE-standardized Penman Monteith equation for a short reference crop (ASCE, 2005) calculated at 30 min time steps, and ET_{OS-24} is the daily (24 h) sum of each $ET_{OS-0.5}$ time step. The Penman-Monteith method provided better agreement between calculated daily ET (scaled from one-time-of-day 30 min ET) and lysimeter-measured daily ET compared with the more commonly used evaporative fraction method (Colaizzi et al., 2006).

FIELD MEASUREMENTS

All field measurements used in this study were obtained at the USDA-ARS Conservation and Production Research Laboratory, Bushland, Texas ($35^{\circ} 11' \text{ N}$, $102^{\circ} 6' \text{ W}$, 1,170 m elevation m.s.l.). The climate is semi-arid with a high evaporative demand of about 2,600 mm per year (Class A pan evaporation) and low precipitation averaging 470 mm per year. The precipitation pattern is bimodal, where most rainfall occurs in mid-spring (i.e., around planting for summer crops) and again in late summer (i.e., around the water-sensitive reproductive stage for summer crops, or prior to planting for winter crops). This pattern has made dryland production feasible for drought-tolerant crops such as cotton, grain sorghum, and winter wheat. Strong advection of heat energy from the south and southwest is typical. The soil is a Pullman clay loam (fine, mixed, super active, thermic torric Paleustolls) with slow permeability, having a dense B2 layer from about 0.15 to 0.40 m depth and a calcic horizon that begins at the 1.1 m depth (USDA-NRCS, 2011).

Evapotranspiration (ET) of four of the region's major crops was measured with large monolithic weighing lysimeters. There were four lysimeters; each lysimeter was located in the center of a 4.7 ha square field (217 m on each side). The fields were arranged in a square pattern and herein are designated NW, SW, NE, and SE. The unobstructed fetch in the predominant wind direction (southwest to south-southwest) is greater than 1 km. The fetch within each lysimeter field was sufficient so that ET measurements were not likely to be influenced by local advection (Tolk et al., 2006). The crops included grain corn (*Zea mays* L.; 1989 season), winter wheat (*Triticum aestivum* L.; 1991-1992 season), grain sorghum (*Sorghum bicolor* L.; 1998 season), and upland cotton (*Gossypium hirsutum* L.; 2008 season) (table 1). Cultural practices were similar to those used for high-yield production in the Southern High Plains. Irrigation was applied with a hose-fed lateral-move sprinkler system. Most crops were planted in raised beds except for winter wheat, which was flat plated. Furrow dikes were installed across raised beds following crop establishment to control runoff and runoff of irrigation and rainfall (Schneider and Howell, 2000). Row orientation was east-west except for the winter wheat (both lysimeters) and

Table 2. Instruments used to measure meteorological variables required for TSEB-N95.

Meteorological Variable	Instrument Manufacturer and Model	Crops Measured
Incident solar irradiance ^[a]	PSP Eppley Laboratory, Inc., Newport, Rhode Island	All
Net radiation	Q*4, REBS, Inc., Seattle, Wash.	Corn
	Q*5.5, REBS, Inc., Seattle, Wash.	Winter wheat, grain sorghum
	Q*7.1, REBS, Inc., Seattle, Wash.	Cotton
Soil heat flux	HF-1 Heat Flux Plates, REBS, Inc., Seattle, Wash.	All
Soil temperature	Thermocouples, Omega Engineering, Inc., Stamford, Conn.	All
Directional brightness temperature	IRT, Everest Interscience, Inc., Tucson, Ariz.	Corn, winter wheat
	IRT/c, Exergen Corp., Watertown, Mass.	Grain sorghum, cotton
Wet/dry bulb air temperature	Aspirated psychrometers designed after Lourence and Pruitt (1969)	Corn, winter wheat
2 m air temperature and RH	MP-100, Rotronics Instrument Corp., Huntington, N.Y.	Grain sorghum
	HMP45, Vaisala, Inc., Boston, Mass.	Cotton
Wind profile (1.0, 1.3, 1.8, and 2.8 m)	014a, Met One Instruments, Inc., Grants Pass, Ore.	Corn, winter wheat
	03101 Wind Sentry, R. M. Young Co., Traverse City, Mich.	Grain sorghum, cotton

^[a] These measurements were obtained from a nearby grass reference site.

cotton crops (NE lysimeter), which were north-south. Row spacing was 0.76 m for corn, cotton, and grain sorghum and 0.25 m for winter wheat. Agronomic details and additional references for each crop are given in table 1.

Each monolithic weighing lysimeter had a surface area of 9.0 m² (3.0 m × 3.0 m) and was 2.4 m deep (Marek et al., 1988), with an accuracy of 0.02 to 0.05 mm d⁻¹ (Howell et al., 1995a). ET was determined by the net change in lysimeter mass, which included losses (evaporation and transpiration) and gains (irrigation, precipitation, dew), divided by the lysimeter area. Lysimeter mass was measured using a load cell (Alphatron S50, 0.5 Hz frequency, Alphatron Industries, Inc., Davie, Fla.; Interface, Inc., Scottsdale, Ariz.) and cantilever system and reported as 30 min averages. Drainage from the lysimeter was maintained with a 10 kPa vacuum pump system, and the drainage effluent was stored in two tanks suspended by separate load cells from the lysimeter. For full cover crops, a small correction factor (1.02) was applied to the lysimeter area to account for the canopy extending to the midpoint between the lysimeter inner and outer walls (9.5 mm wall thickness and 10 mm air gap). The 30 min ET averages were summed to daily (24 h) totals.

Each lysimeter site included a mast located at the midpoint of the north edge that contained micrometeorological instruments. Measurements used in this study included net radiation (R_N), soil heat flux (G), soil temperature (T_S), air temperature (T_A), wet bulb temperature (T_W) (or relative humidity, RH), wind speed (U), and the directional brightness temperature (T_B) (Norman and Becker, 1995) of the lysimeter surface (table 2). Measurements were made at 6 s intervals and reported as 30 min averages, simultaneously with lysimeter mass measurements. All measurements, including lysimeter mass, were recorded and averaged by a CR-7X data logger (Campbell Scientific, Inc., Logan, Utah). Global shortwave incoming solar irradiance (R_S) was measured at a site immediately east of the SE lysimeter field that was planted in tall fescue since 1995 (Howell et al., 2000). R_N , T_A , T_W (or RH), U , and T_B were typically measured at a 2.0 m height above the soil surface. Surface G was calculated using a procedure described by Evett et al. (2012), which requires near-surface measurements of G and soil temperature, and measurements or calculation of soil water content. Briefly, G was measured by soil heat

flux plates buried at 50 mm below the surface, and soil heat storage was calculated from measurements of the average soil temperature by thermocouples buried at 10 and 40 mm near the soil heat flux plates. There were four soil heat flux plate and thermocouple sets, with two positioned beneath adjacent crop rows and two beneath adjacent interrows. Soil water content to the 50 mm depth was calculated using a simple soil water balance and evaporation model (Allen et al., 1998), in which the lower and upper limits of near-surface soil water were taken as 0.05 to 0.30 m³ m⁻³, respectively, which was verified by time-domain reflectometry (TDR) measurements during the 2008 cotton season (Evett et al., 2012).

T_B was measured with stationary infrared thermometers (IRTs) viewing the lysimeter surface at a 30° zenith angle (θ_R) and an azimuth toward the southwest (45° for corn and 60° for other crops from due south; Huband and Monteith, 1986), with a 2:1 field-of-view. Since corn, grain sorghum, and cotton (SE lysimeter field only) had an east-west row orientation, the radiometer azimuth angle relative to the crop row (Φ_R , where $\Phi_R = 0^\circ$ viewing parallel to the row, and $\Phi_R = 90^\circ$ viewing perpendicular to the row) was 45° for corn and 30° for grain sorghum and cotton (SE lysimeter). Similarly, cotton (NE lysimeter field only) and winter wheat had a north-south row orientation; therefore, $\Phi_R = 60^\circ$. Everest IRT model series 4000 (Everest Interscience, Inc., Tucson, Ariz.) were used for corn and winter wheat; Exergen IRT model IRT/c (Exergen Corp., Watertown, Mass.) were used for grain sorghum and cotton. The Everest IRTs were factory calibrated annually, and the Exergen IRTs were calibrated using an Everest model 1000 black body or an Omega Black Point BB701 black body (Omega Engineering, Inc., Stamford, Conn.). The Exergen IRTs did not feature a chopper or detector temperature measurement; therefore, they were insulated from the outside air to reduce the influence of longwave radiation variability from the internal body cavity on the detector. The insulation was made of two concentric white PVC reducers (30 mm total thickness); a white PVC cap (16 mm total thickness) sealed the end opposite the IRT opening. It is not known to what extent the lack of detector temperature for the Exergen IRTs may have degraded the accuracy of calibration (Kalma et al., 1988; Bugbee et al., 1998); however, no differences in TSEB-N95 model performance were apparent between the

IRT manufacturers. The use of ground-based IRTs was nonetheless deemed advantageous over aircraft or satellite data because atmospheric correction was not required and 30 min measurements were available. Directional radiometric surface temperature (T_R) was calculated by subtracting the reflected atmospheric longwave radiation from the contribution to T_B (Norman and Becker, 1995), where longwave reflectance was assumed equal to the bulk (soil and canopy) surface emittance, which was assumed to be 0.98. Soil emittance equal to 0.98 was verified by measurements over bare soil using a Cimel CE 312 multiband thermal radiometer (Cimel Electronique, Paris, France), and canopy emittance equal to 0.98 was assumed based on Idso et al. (1969) and Campbell and Norman (1998). Atmospheric emittance was calculated using the Brutsaert (1982) equation.

Plant measurements and destructive samples were obtained at six to ten dates during the growing season spanning from the early vegetative stage to physiological maturity at 1.0 to 1.5 m² sites about 10 to 20 m from the lysimeters. Leaf area was measured with a leaf area meter (model LI-3100, Li-Cor, Lincoln, Neb.), and the meter accuracy was verified periodically with a 0.005 m² standard disk. Plant height (h_C) and leaf area index (LAI) were related to growing degree days (GDD) by linear interpolation so that these parameters could be calculated between sample dates. GDD was calculated as:

$$\text{GDD} = \frac{\max(T_{A,\min}, T_{base}) + \min(T_{A,\max}, T_{peak})}{2} - T_{base} \quad (6)$$

where $T_{A,\min}$ and $T_{A,\max}$ are the minimum and maximum, respectively, daily air temperatures, T_{base} is the lower air temperature limit at which a crop will develop, T_{peak} is the upper air temperature limit at which a crop will accumulate GDD (i.e., air temperatures greater than T_{peak} will not increase GDD), and T_{base} and T_{peak} are crop-specific (table 1). All variables have °C units. The TSEB-N95 model was evaluated for a fairly wide range of h_C and LAI, from early development to maturity and senescence.

Data were restricted to clear-sky days, when measured R_S closely matched ($r^2 \geq 0.98$) theoretical clear sky irradiance (ASCE, 2005) to ensure relatively steady-state energy fluxes. Data were excluded when T_A was below freezing, which included several days during the winter wheat season. Data were not used during days when irrigation, precipitation, plant measurements, or instrument maintenance and repair occurred.

MODEL EVALUATION

The TSEB-N95 model was evaluated by comparing calculated daily ET with daily ET measured by the weighing lysimeters. Agreement between calculated vs. measured daily ET was assessed by root mean square error (RMSE), mean absolute error (MAE), mean bias error (MBE), and the modified coefficient of model efficiency (E_C), where $-\infty < E_C \leq 1.0$, with greater E_C values indicating better model agreement (Legates and McCabe, 1999). If $E_C \leq 0$, then the mean of all measurements is actually a better calculation

compared with the model. The E_C is a non-squared version of the original Nash and Sutcliffe (1970) model efficiency parameter, which Legates and McCabe (1999) argued was less sensitive to outliers. The extent to which RMSE is greater than MAE is related to outliers in calculated vs. measured scatter. Additional parameters reported were the calculated vs. measured slope, intercept, and coefficient of determination (r^2).

In addition to daily ET, agreement between calculated vs. instantaneous net radiation (R_N), soil heat flux (G), and latent heat flux (LE) were assessed. Measured LE was derived by converting 30 min ET averages (12:30 to 13:00 CST) measured by the lysimeters. R_N , G , LE, and ET were initially calculated using TSEB-N95 in which the nonrandom spatial distribution of row crop vegetation was accounted for using the clumping index approach (Kustas and Norman, 1999; Anderson et al., 2005). For comparison, R_N , G , LE, and ET were calculated using a modified form of TSEB-N95 in which the nonrandom spatial distribution of row crop vegetation was accounted for by modeling the rows as elliptical hedgerows (Colaizzi et al., 2010, 2012a, 2012b). Agreement between measured and calculated energy fluxes (R_N , G , and LE) were assessed using the average of 12:30 to 13:00 (i.e., 30 min average during solar noon). Data were pooled for all four crops (corn, cotton, grain sorghum, and winter wheat).

The TSEB-N95 model was evaluated under a wide range of climatic conditions, which may occur within just a few days in continental climates such as Bushland, Texas. Most days evaluated occurred during the summer crop growing season (late spring to mid-autumn), although winter wheat included some days during winter or early spring when the air temperature was slightly above freezing. Wind speed measured at 2 m above the soil surface averaged 3.4 to 5.4 m s⁻¹. The greatest wind runs typically occurred during spring (March, April, and May), and the least occurred during late summer (around August).

RESULTS AND DISCUSSION

The wide ranges of canopy height (h_C) and leaf area index (LAI) evaluated resulted in a wide range of the fraction of vegetation appearing in the infrared thermometer field of view (f_{VR}) for each crop, which was desirable in order to evaluate the TSEB-N95 model (fig. 2). The value of f_{VR} using the clumping index and elliptical hedgerow approaches was similar for corn for the entire range of f_{VR} (i.e., near zero to one), but f_{VR} was different for cotton, grain sorghum, and winter wheat. This was mainly related to the elliptical hedgerow approach having a greater sensitivity to the radiometer zenith (θ_R) and azimuth (Φ_R) view angle compared with the clumping index approach, where increases in θ_R (i.e., more horizontal view) and Φ_R (i.e., view more perpendicular to the crop rows) resulted in f_{VR} increasing more rapidly for the elliptical hedgerow compared with the clumping index (Colaizzi et al., 2010). The elliptical hedgerow approach often resulted in greater f_{VR} compared with the clumping index approach for winter wheat (north-south rows, $\Phi_R = 60^\circ$) but consistently smaller f_{VR} for grain sor-

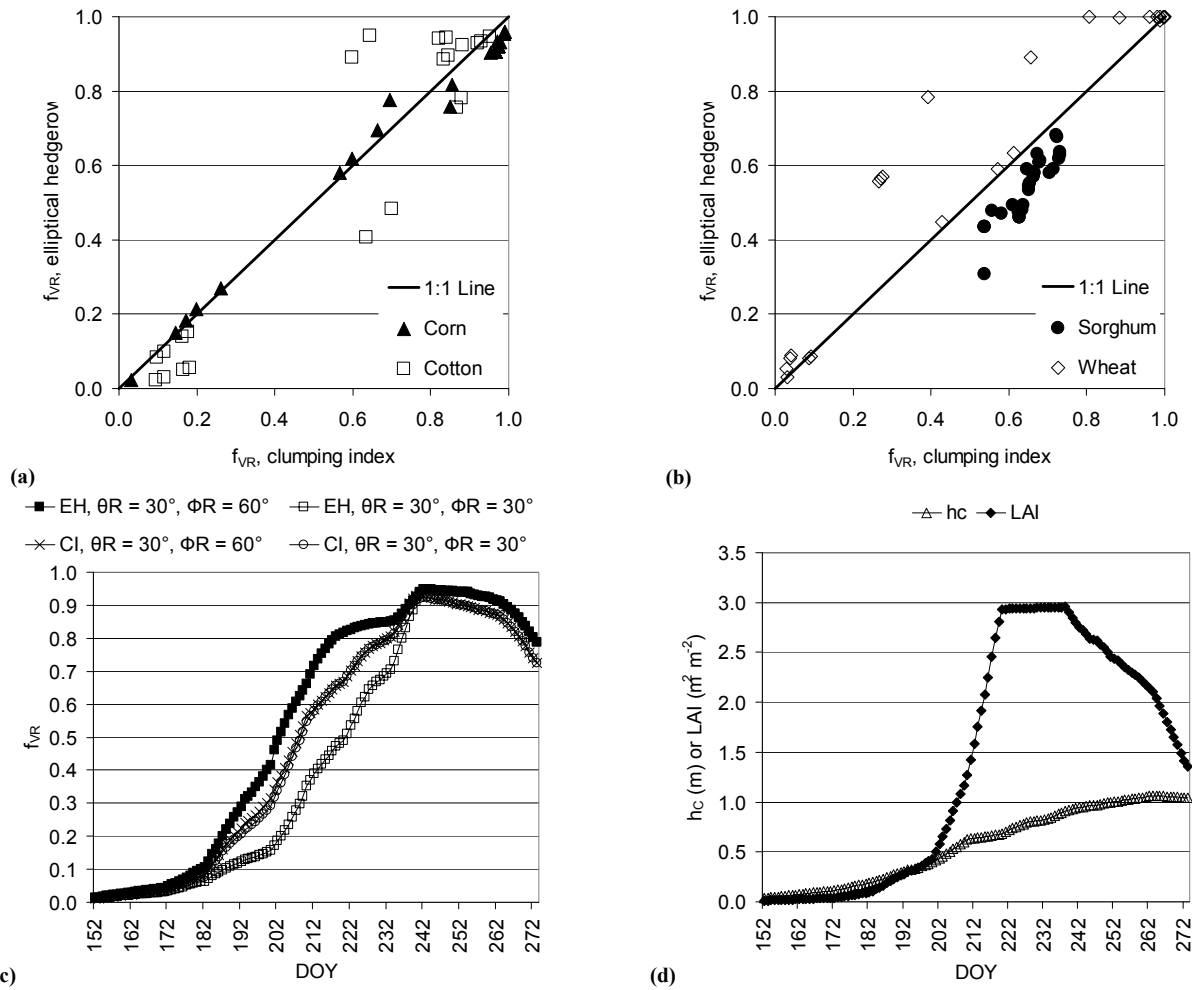


Figure 2. Comparison of the fraction of vegetation appearing in the radiometer field of view (f_{VR}) using the clumping index and elliptical hedgerow approaches for (a) corn and cotton and (b) sorghum and wheat, (c) example of day-of-year (DOY) time series f_{VR} of both approaches for cotton with constant radiometer zenith view angle (θ_R) but different radiometer azimuth view angle (Φ_R), and (d) corresponding canopy height (h_c) and leaf area index (LAI) of cotton example.

ghum (east-west rows, $\Phi_R = 30^\circ$). Similarly for cotton, f_{VR} was larger for the elliptical hedgerow compared with the clumping index in the NE lysimeter field (north-south rows, $\Phi_R = 60^\circ$) but smaller in the SE lysimeter field (east-west rows, $\Phi_R = 30^\circ$) for mid-range f_{VR} values. The responses of both approaches to different Φ_R is also shown in the f_{VR} time series for the cotton season (fig. 2c), with corresponding h_c and LAI (fig. 2d). From around day of year (DOY) 182 to 232, h_c ranged from 0.2 to 0.8 m, LAI ranged from 0.3 to 2.95 $m^2 m^{-2}$, and the elliptical hedgerow was greater than the clumping index when $\Phi_R = 60^\circ$, but less when $\Phi_R = 30^\circ$. However, the two different Φ_R values resulted in little differences in f_{VR} calculated by the clumping index throughout the season, and little differences in f_{VR} calculated by the elliptical hedgerow when $h_c < 0.1$ m or $h_c > 0.8$ m. Student t-tests for paired samples (i.e., clumping index vs. elliptical hedgerow) were all < 0.01 except for corn, which was 0.82.

As expected, the clumping index and elliptical hedgerow approaches also resulted in different partitioning of net radiation (R_N) to the canopy ($R_{N,C}$) and soil ($R_{N,S}$) components around solar noon (fig. 3). This was mainly related to differences in direct-beam shortwave irradiance intercepted by

the canopy, in that assumptions about canopy structure would be expected to have a greater impact on direct-beam compared with diffuse components (Campbell and Norman, 1998). $R_{N,C}$ tended to be greater for corn, cotton, and winter wheat using the elliptical hedgerow approach (Student t-tests for paired samples were all < 0.01) but was inconsistent for grain sorghum (Student t-test = 0.99). However, $R_{N,S}$ was usually less for all crops for the elliptical hedgerow approach compared with the clumping index (all Student t-tests were < 0.01). When canopy cover was very sparse (resulting in low $R_{N,C}$ and large $R_{N,S}$), there were little differences with either approach.

Agreement between calculated and measured total net radiation (R_N) near solar noon was very similar using both the clumping index (table 3) and elliptical hedgerow (table 4) approaches, with the latter approach giving slightly better agreement. Overall errors between calculated and measured R_N was somewhat greater compared with other studies that investigated TSEB-N95; for example, Kustas and Norman (1999, 2000) and Li et al. (2005) reported RMSE and MAE ranging from 17 to 21 $W m^{-2}$. However, errors as a percent of the measured mean in the present study were similar to other TSEB-N95 studies. The larger RMSE and MAE reported in

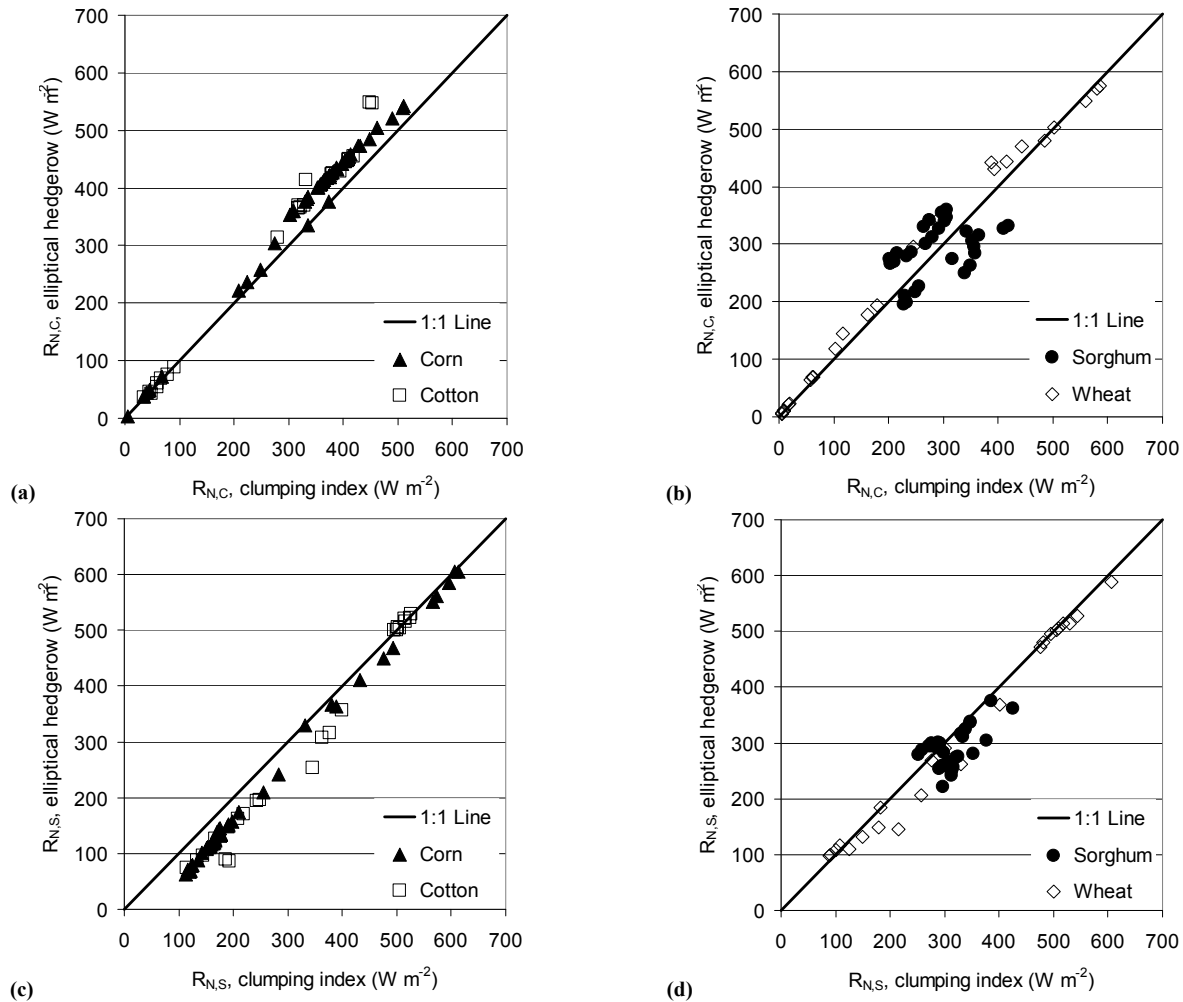


Figure 3. Comparison of the clumping index and elliptical hedgerow approaches in calculating net radiation to the canopy ($R_{N,C}$) for (a) corn and cotton and (b) sorghum and wheat, and comparison of the two approaches in calculating net radiation to the soil ($R_{N,S}$) for (c) corn and cotton and (d) sorghum and wheat.

the present study may have been related to a larger range of R_N measurements (resulting from the larger range of canopy cover) compared with other studies, as well as inconsisten-

cies in measurements reported by net radiometers, which have been shown to vary by manufacturer and model (Kustas et al., 1998; Blonquist et al., 2009).

Table 3. Statistical parameters of agreement between measured and calculated net radiation (R_N), soil heat flux (G), and latent heat flux (LE), average of 12:30 to 13:00 CST, and daily evapotranspiration (ET) using the clumping index approach ($n = 121$).

Statistic ^[a]	R_N ($W m^{-2}$)	G ($W m^{-2}$)	LE ($W m^{-2}$)	ET ($mm d^{-1}$)
Measured mean	596	73.2	350	4.62
Measured SD	81.8	40.3	191	2.63
Calculated mean	595	73.44	352	4.72
Calculated SD	80.8	41.8	186	2.71
Slope	0.88	0.60	0.89	0.96
Intercept	68.9	29.3	39.9	0.28
r^2	0.80	0.34	0.84	0.87
E_C	0.56	0.18	0.60	0.59
RMSE	37.2	37.4	76.8	1.00
% RMSE of measured mean	6.3%	51%	22%	22%
MAE	29.4	26.8	59.8	0.79
% MAE of measured mean	4.9%	37%	17%	17%
MBE	-0.59	0.23	2.4	0.093
% MBE of measured mean	-0.10%	0.32%	0.67%	2.0%

^[a] SD = standard deviation, E_C = modified model efficiency, RMSE = root mean square error, MAE = mean absolute error, and MBE = mean bias error.

Table 4. Statistical parameters of agreement between measured and calculated net radiation (R_N), soil heat flux (G), and latent heat flux (LE), average of 12:30 to 13:00 CST, and daily evapotranspiration (ET) using the elliptical hedgerow approach ($n = 121$).

Statistic ^[a]	R_N ($W m^{-2}$)	G ($W m^{-2}$)	LE ($W m^{-2}$)	ET ($mm d^{-1}$)
Measured mean	596	73.2	350	4.62
Measured SD	81.8	40.3	191	2.63
Calculated mean	596	66.3	358	4.79
Calculated SD	81.1	43.1	184	2.70
Slope	0.91	0.64	0.90	0.98
Intercept	51.4	19.6	42.9	0.28
r^2	0.85	0.36	0.87	0.90
E_C	0.63	0.17	0.65	0.64
RMSE	32.0	38.0	68.5	0.86
% RMSE of measured mean	5.4%	52%	20%	19%
MAE	24.7	27.2	53.0	0.69
% MAE of measured mean	4.1%	37%	15%	15%
MBE	0.43	-6.9	8.3	0.17
% MBE of measured mean	0.073%	-9.4%	2.4%	3.6%

^[a] SD = standard deviation, E_C = modified model efficiency, RMSE = root mean square error, MAE = mean absolute error, and MBE = mean bias error.

Surface soil heat flux (G) calculated as a function of soil net radiation ($R_{N,S}$) (eq. 2) near solar noon agreed poorly with surface G derived from soil heat flux plates and thermocouples, using both the clumping index (table 3) and elliptical hedgerow (table 4) approaches, in terms of E_C , RMSE, and MAE. However, MBE using the clumping index was small ($<1 \text{ W m}^{-2}$). The elliptical hedgerow, on the other hand, tended to under-calculate G , which was consistent with $R_{N,S}$ tending to be smaller using this approach compared with the clumping index (fig. 3b). The generally large errors may have been related to inadequate sampling of G , since only two soil heat flux plate and thermocouple locations were available, and G has been shown to vary considerably beneath row crops due to variation of sunlit and shaded soil (e.g., Ham and Kluitenberg, 1993). The errors would have been even larger if G had been calculated as a constant fraction of $R_{N,S}$ compared with accounting for the phase difference between $R_{N,S}$ and G using equation 2 (data not shown). A more detailed study of G and how it varies across crop rows and interrows is presently underway at our study location, where ten soil heat flux plates and thermocouples were deployed within adjacent crop rows, with preliminary results given by Evett et al. (2012) and Agam et al. (2012).

Calculated latent heat flux (LE) agreed fairly well with LE derived from lysimeters measurements using both the clumping index (table 3) and elliptical hedgerow (table 4) approaches, with the latter approach resulting in slightly less RMSE and MAE but greater MBE. The greater MBE for the elliptical hedgerow may have resulted from under-calculations of G , leading to over-calculations of available energy and hence turbulent fluxes. This was related to differences in $R_{N,C}$ and $R_{N,S}$ partitioning, as noted previously. For both approaches, the magnitudes of RMSE and MAE were substantially greater compared with those reported in previous TSEB-N95 studies where infrared thermometers were used, which were 31 to 55 W m^{-2} (Norman et al., 1995; Kustas and Norman, 1999, 2000; Li et al., 2005). However, in the present study, RMSE as a percentage of the measured mean was similar to those reported in previous TSEB-N95 studies, which were around 20% to 30%. Hence, the greater magnitude of RMSE and MAE in the present study was in part due to the much greater LE resulting from strong regional advection, high solar irradiance, and high vapor pressure deficit at the study location.

Agreement between calculated and measured daily ET followed very similar trends as LE, which was expected since calculated daily ET was derived from calculated LE (tables 3 and 4). Both the clumping index and elliptical hedgerow approaches resulted in RMSE and MAE within 1.0 mm d^{-1} and MBE less than 0.20 mm d^{-1} . The elliptical hedgerow approach resulted in slightly less scatter compared with the clumping index approach for most of the range of ET measurements (fig. 4). Although the differences between the two approaches were marginal and could have been related to compensating errors in the energy balance, this result was consistent with previous studies, where the elliptical hedgerow resulted in better agreement with f_{VR} measured with digital photography (Colaizzi et al., 2010), as well as better agreement with measurements of transmit-

ted and reflected shortwave radiation (Colaizzi et al., 2012b) compared with the clumping index.

For the lower range of ET values (i.e., $<3 \text{ mm d}^{-1}$), the clumping index and elliptical hedgerow approaches both resulted in over-calculations of ET for grain sorghum and winter wheat, but both approaches tended to under-calculate ET for corn (fig. 4). This occurred mainly later in the season when f_{VR} began to include non-transpiring plant components, leaves began to senesce, and bulk canopy resistance would be expected to increase. The TSEB-N95 model contains two provisions to account for this indirectly, which are to decrease the fraction of green LAI, and to reduce the Priestley-Taylor parameter (α_{PT}) below the typical value of 1.3. Both provisions result in increasing the canopy temperature (T_C) and sensible heat flux (H) away from the surface, and reducing LE and ET. In order to simplify model diagnostics, the fraction of green LAI was not reduced in the present study (although a rational procedure could have been developed, such as basing this on red and near-infrared reflectance measurements). However, TSEB-N95 did reduce α_{PT} to between 0.8 and 1.2 for winter wheat and grain sorghum, but this still resulted in over-calculations in LE and ET. In a previous study where ET was calculated with TSEB-N95 for spring wheat, French et al. (2007) also reported over-calculations that became greater toward the end of the season as leaves senesced, although they used a constant $\alpha_{PT} = 1.26$. In the present study, reducing α_{PT} resulted in ET under-calculations for corn later in the season, in contrast to grain sorghum and winter wheat. This mainly occurred when vapor pressure deficit was relatively low (i.e., 0.5 to 1.5 kPa; more typical values being 2 to 5 kPa). However, if α_{PT} was not reduced, then late season LE and ET under-calculations for corn were largely mitigated, but late season LE and ET over-calculations for wheat and grain sorghum were exacerbated (data not shown). These results clearly point to a need to improve calculations of T_C , especially late in the season when the assumptions in the Priestley-Taylor approximation begin to deteriorate. Although French et al. (2007) pointed out that, for the purposes of irrigation scheduling, ET model accuracy later in the season after irrigation is terminated is not as important, it would be nonetheless desirable to achieve consistent model accuracy throughout the season and during fallow periods in order to calculate the soil water balance.

Several days included ET measurements between 8 and 16 mm d^{-1} , which occurred for corn, cotton, and winter wheat (fig. 4). For each crop, the largest ET values occurred during mid-season when canopy cover was complete and on days of strong regional advection. Wind speeds at the 2 m height were from 5 to 8 m s^{-1} , vapor pressure deficits were greater than 2 kPa, and advected energy contributed up to 30% toward LE, which was similar to that reported by Tolk et al. (2006) for irrigated alfalfa at this location. Daily ET was calculated fairly well using both the clumping index and elliptical hedgerow approaches, with errors less than 1.0 mm d^{-1} for the latter approach. This suggests that measurements of directional brightness temperature and air temperature directly over the crop can be used to calculate advected energy contributing to ET with

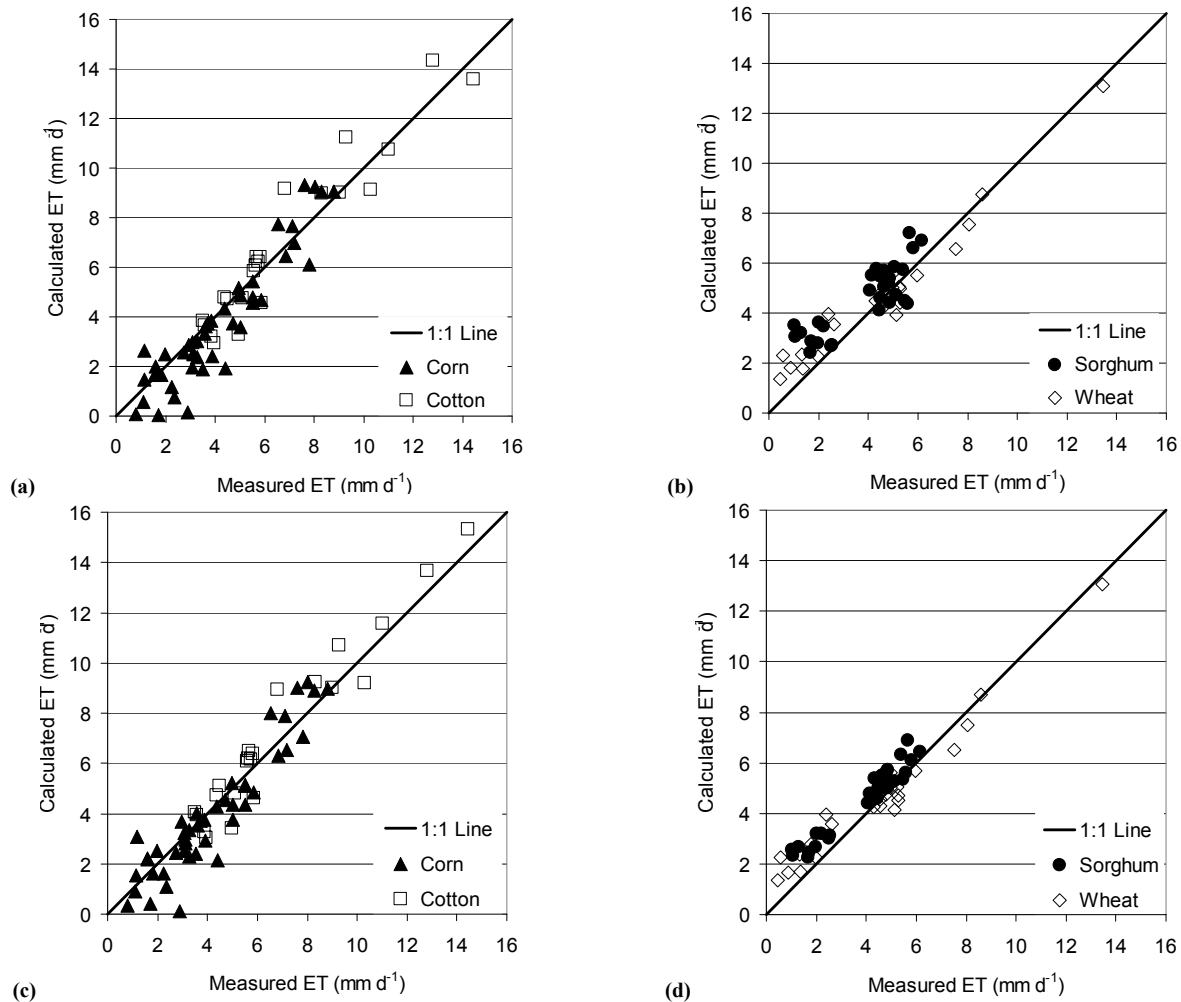


Figure 4. Comparison of calculated vs. measured daily evapotranspiration (ET) using different approaches for accounting for the nonrandom spatial distribution of vegetation: (a) clumping index for corn and cotton, (b) clumping index for sorghum and wheat, (c) elliptical hedgerow for corn and cotton, and (d) elliptical hedgerow for sorghum and wheat. See tables 3 and 4 for statistical parameters of agreement.

acceptable accuracy in TSEB-N95. However, it should be noted that in most practical applications, measurements of air temperature are usually only available at agricultural weather stations, which may not be representative of all crop conditions. To what extent this could degrade TSEB-N95 performance was beyond the scope of this study, but it will be addressed in future studies; a procedure described by Norman et al. (2000) has been shown to reduce errors using surface and air temperature measurements at two times of day.

The recent availability and standardization of wireless technology have led to the development of stationary and moving ground-based remote sensing platforms designed for real-time irrigation management (e.g., Mahan et al., 2010; O'Shaughnessy and Evett, 2010a), where TSEB-N95 would have immediate application. Remote sensing platforms must meet several requirements to be useful for agricultural management, including a spatial resolution of a few meters, a repeat frequency of a few days, and a turnaround time (i.e., the time interval from field measurement to final information) on the order of minutes (Jackson, 1984). Although airborne and satellite platforms generally provide greater areal coverage, only ground-based systems

developed recently can potentially meet all of the requirements described by Jackson (1984). At least one stationary, wireless, ground-based remote sensing system has been commercialized (Mahan et al., 2010). Self-propelled irrigation systems (i.e., center pivot and lateral move) can provide a mobile sensor platform, reducing the number of sensors required, because these systems pass over fields at regular intervals (e.g., O'Shaughnessy and Evett, 2010b; O'Shaughnessy et al., 2012). Self-propelled irrigation systems are used on nearly 50% of the 23 million ha of irrigated land in the U.S. and on nearly 80% of the irrigated land in the Southern High Plains, with continued adoption expected (USDA-NASS, 2008). Therefore, these systems may be amenable for more widespread adoption of ground-based remote sensing, which could provide the data required to drive algorithms such as TSEB-N95, and provide real-time feedback information required to implement advanced irrigation management and automation strategies.

CONCLUSION

Daily evapotranspiration (ET) was calculated using a thermal-based two-source energy balance model (TSEB-

N95) developed by Norman et al. (1995) for four crops and compared to ET measured by large, monolithic, weighing lysimeters in Bushland, Texas. Crops included corn, cotton, grain sorghum, and winter wheat. The TSEB-N95 model was evaluated using two methods of accounting for the nonrandom spatial distribution of row crops: the widely used clumping index approach, and an approach in which crop rows were modeled as elliptical hedgerows. Each approach resulted in different partitioning of energy flux components to the soil and canopy, and the elliptical hedgerow approach resulted in slightly better ET calculation. Root mean square error (RMSE), mean absolute error (MAE), and mean bias error (MBE) were 1.0 (22%), 0.79 (17%), and 0.093 (2.0%) mm d⁻¹ (percentage of measured mean of 4.62 mm d⁻¹), respectively, using the clumping index approach. RMSE, MAE, and MBE were 0.86 (19%), 0.69 (15%), and 0.17 (3.6%) mm d⁻¹, respectively, using the elliptical hedgerow approach. These error rates were similar to those reported in previous studies, although the present study was conducted for a wider range of vegetation cover and climatic conditions. Given the possible sources of error inherent in thermal energy balance models, especially uncertainties in estimating soil heat flux, the fraction of canopy cover, leaf area index, and surface-to-air temperature gradients, the performance of TSEB-N95 in estimating ET was deemed acceptable. Additional refinements to TSEB-N95 are presently underway for estimating initial canopy temperature, resistance components, and soil heat flux. Future studies will apply TSEB-N95 with the elliptical hedgerow approach using wireless radiometers aboard center-pivot machines to calculate ET, with the aim of providing producers remote sensing tools that will reduce management time and enhance water and energy conservation.

ACKNOWLEDGEMENTS

This research was supported by the USDA-ARS National Program 211, Water Availability and Watershed Management, and by the USDA-ARS Ogallala Aquifer Program, a consortium between the USDA-ARS, Kansas State University, Texas AgriLife Research, Texas AgriLife Extension Service, Texas Tech University, and West Texas A&M University. We are grateful to Dr. Andrew French, USDA-ARS, Maricopa, Arizona, for allowing us to use the Cimel multiband thermal radiometer and for his critical review of the manuscript. We also thank the numerous biological technicians and student workers for their meticulous and dedicated efforts in executing experiments and obtaining and processing data.

REFERENCES

Agam, N., W. P. Kustas, M. C. Anderson, J. M. Norman, P. D. Colaizzi, T. A. Howell, J. H. Prueger, T. P. Meyers, and T. B. Wilson. 2010. Application of the Priestley-Taylor approach in a two-source surface energy balance model. *J. Hydrometeorol.* 11(2): 185-198.

Agam, N., W. P. Kustas, S. R. Evett, P. D. Colaizzi, M. Cosh, and L. G. McKee. 2012. Soil heat flux variability influenced by row direction in irrigated cotton. *Adv. Water Resour.* (in review).

Allen, R. G., L. S. Periera, D. Raes, and M. Smith. 1998. Crop evapotranspiration: Guidelines for computing crop water requirements. Irrigation and Drainage Paper No. 56. Rome, Italy: United Nations FAO.

Anderson, M. C., J. M. Norman, W. P. Kustas, F. Li, J. H. Prueger, and J. R. Mecikalski. 2005. Effects of vegetation clumping on two-source model estimates of surface energy fluxes from an agricultural landscape during SMACEX. *J. Hydrometeorol.* 6(6): 892-909.

ASCE. 2005. *The ASCE Standardized Reference Evapotranspiration Equation*. R. G. Allen, I. A. Walter, R. L. Elliot, T. A. Howell, D. Itenfisu, M. E. Jensen, and R. L. Snyder, eds. Reston, Va.: ASCE.

Blonquist, J. M., Jr., B. D. Tanner, and B. Bugbee. 2009. Evaluation of measurement accuracy and comparison of two new and three traditional net radiometers. *Agric. Forest Meteorol.* 149(10): 1709-1721.

Brutsaert, W. 1982. *Evaporation into the Atmosphere*. Dordrecht, The Netherlands: Kluwer.

Bugbee, B., M. Droter, O. Monje, and B. Tanner. 1998. Evaluation and modification of commercial infrared transducers for leaf temperature measurement. *Adv. Space Res.* 22(10): 1425-1434.

Campbell, G. S., and J. M. Norman. 1998. *An Introduction to Environmental Biophysics*. 2nd ed. New York, N.Y.: Springer-Verlag.

Chavez, J. L., T. A. Howell, and K. S. Copeland. 2009. Evaluating eddy covariance cotton ET measurements in an advective environment with large weighing lysimeters. *Irrig. Sci.* 28(1): 35-50.

Chen, J. M., and J. Cihlar. 1995. Quantifying the effect of canopy architecture on optical measurements of leaf area index using two gap size analysis methods. *IEEE Trans. Geosci. Remote Sens.* 33(3): 777-787.

Colaizzi, P. D., S. R. Evett, T. A. Howell, and J. A. Tolk. 2006. Comparison of five models to scale daily evapotranspiration from one-time-of-day measurements. *Trans. ASABE* 49(5): 1409-1417.

Colaizzi, P. D., S. A. O'Shaughnessy, P. H. Gowda, S. R. Evett, T. A. Howell, W. P. Kustas, and M. C. Anderson. 2010. Radiometer footprint model to estimate sunlit and shaded components for row crops. *Agron. J.* 102(3): 942-955.

Colaizzi, P. D., S. R. Evett, T. A. Howell, F. Li, W. P. Kustas, and M. C. Anderson. 2012a. Radiation model for row crops: I. Geometric model description and parameter optimization. *Agron. J.* 104(2): 225-240.

Colaizzi, P. D., R. C. Schwartz, S. R. Evett, T. A. Howell, P. H. Gowda, and J. A. Tolk. 2012b. Radiation model for row crops: II. Model evaluation. *Agron. J.* 104(2): 241-255.

Evans, R. G., and B. A. King. 2010. Site-specific sprinkler irrigation in a water limited future. In *Proc. 5th Natl. Dec. Irrig. Conf.* ASABE Paper No. IRR108491. St. Joseph, Mich.: ASABE.

Evett, S. R., T. A. Howell, A. D. Schneider, K. S. Copeland, and D. A. Dusek. 1994. Energy and water balance modeling of winter wheat. ASAE Paper No. 942022. St. Joseph, Mich.: ASAE.

Evett, S. R., N. Agam, W. P. Kustas, P. D. Colaizzi, and R. C. Schwartz. 2012. Soil profile method for soil thermal diffusivity, conductivity, and heat flux: Comparison to soil heat flux plates. *Adv. Water Resour.* (in review).

French, A. N., D. J. Hunsaker, T. R. Clarke, G. J. Fitzgerald, W. E. Lockett, and P. J. Pinter Jr. 2007. Energy balance estimation of evapotranspiration for wheat grown under variable management practices in central Arizona. *Trans. ASABE* 50(6): 2059-2071.

Ham, J. M., and G. J. Kluitenberg. 1993. Positional variation in the soil energy balance beneath a row-crop canopy. *Agric. Forest Meteorol.* 63(1-2): 73-92.

- Howell, T. A., A. D. Schneider, D. A. Dusek, T. H. Marek, and J. L. Steiner. 1995a. Calibration and scale performance of Bushland weighing lysimeters. *Trans. ASAE* 38(4): 1019-1024.
- Howell, T. A., J. L. Steiner, A. D. Schneider, and S. R. Evett. 1995b. Evapotranspiration of irrigated winter wheat: Southern High Plains. *Trans. ASAE* 38(3): 745-759.
- Howell, T. A., J. L. Steiner, A. D. Schneider, S. R. Evett, and J. A. Tolk. 1997. Seasonal and maximum daily evapotranspiration of irrigated winter wheat, sorghum, and corn: Southern High Plains. *Trans. ASAE* 40(3): 623-634.
- Howell, T. A., S. R. Evett, A. D. Schneider, D. A. Dusek, and K. S. Copeland. 2000. Irrigated fescue grass ET compared with calculated reference grass ET. In *Proc. 4th Dec. Natl. Irrig. Symp.*, 228-242. St. Joseph, Mich.: ASAE.
- Howell, T. A., S. R. Evett, J. A. Tolk, and A. D. Schneider. 2004. Evapotranspiration of full-, deficit-irrigated, and dryland cotton on the northern Texas High Plains. *J. Irrig. Drain. Eng.* 130(4): 277-285.
- Huband, N. D. S., and J. L. Monteith. 1986. Radiative surface temperature and energy balance of a wheat canopy: I. Comparison of radiative and aerodynamic canopy temperature. *Boundary-Layer Meteorol.* 36(1-2): 1-17.
- Idso, S. B., R. D. Jackson, W. L. Ehrler, and S. T. Mitchell. 1969. A method for determination of infrared emittance of leaves. *Ecology* 50(5): 899-902.
- Jackson, R. D. 1984. Remote sensing of vegetation characteristics for farm management. *SPIE* 475: 81-96.
- Kalma, J. D., H. Alknsnis, and G. P. Laughlin. 1988. Calibration of small infrared surface temperature transducers. *Agric. Forest Meteorol.* 43(1): 83-98.
- Kustas, W. P. 1990. Estimates of evapotranspiration with a one- and two-layer model of heat transfer over partial canopy cover. *J. Appl. Meteorol.* 29(8): 704-715.
- Kustas, W. P., and J. M. Norman. 1999. Evaluation of soil and vegetation heat flux predictions using a simple two-source model with radiometric temperatures for partial canopy cover. *Agric. Forest Meteorol.* 94(1): 13-29.
- Kustas, W. P., and J. M. Norman. 2000. A two-source energy balance approach using directional radiometric temperature observations for sparse canopy covered surfaces. *Agron. J.* 92(8): 847-854.
- Kustas, W. P., J. H. Prueger, L. E. Hipps, J. L. Hatfield, and D. Meek. 1998. Inconsistencies in net radiation estimates from use of several models of instruments in a desert environment. *Agric. Forest Meteorol.* 90(4): 257-263.
- Kustas, W. P., J. M. Norman, T. J. Schmugge, and M. C. Anderson. 2004. Mapping surface energy fluxes with radiometric temperature. In *Thermal Remote Sensing in Land Surface Processes*, 205-254. New York, N.Y.: CRC Press.
- Legates, D. R., and G. J. McCabe Jr. 1999. Evaluating the use of "goodness-of-fit" measures in hydrologic and hydroclimatic model validation. *Water Resources Res.* 35(1): 233-241.
- Li, F., W. P. Kustas, J. H. Prueger, C. M. U. Neale, and T. J. Jackson. 2005. Utility of remote sensing-based two-source energy balance model under low- and high-vegetation cover conditions. *J. Hydrometeorol.* 6(6): 878-891.
- Lourence, F. J., and W. O. Pruitt. 1969. A psychrometer system for micrometeorology profile determination. *J. Appl. Meteorol.* 8(4): 492-498.
- Mahan, J. R., W. Conaty, J. Neilsen, P. Payton, and S. B. Cox. 2010. Field performance in agricultural settings of a wireless temperature monitoring system based on a low-cost infrared sensor. *Comp. Elec. Agric.* 71(2): 176-181.
- Marek, T. H., A. D. Schneider, T. A. Howell, and L. L. Ebeling. 1988. Design and construction of large weighing monolithic lysimeters. *Trans. ASAE* 31(2): 477-484.
- Nash, J. E., and J. V. Sutcliffe. 1970. River flow forecasting through conceptual models: I. A discussion of principles. *J. Hydrol.* 10(3): 282-290.
- Norman, J. M., and F. Becker. 1995. Terminology in thermal infrared remote sensing of natural surfaces. *Remote Sensing Rev.* 12(3-4): 159-173.
- Norman, J. M., W. P. Kustas, and K. S. Humes. 1995. A two-source approach for estimating soil and vegetation energy fluxes from observations of directional radiometric surface temperature. *Agric. Forest Meteorol.* 77(3-4): 263-293.
- Norman, J. M., W. P. Kustas, J. H. Prueger, and G. H. Diak. 2000. Surface flux estimation using radiometric temperature: A dual-temperature-difference method to minimize measurement errors. *Water Resources Res.* 36(8): 2263-2274.
- O'Shaughnessy, S. A., and S. R. Evett. 2010a. Developing wireless sensor networks for monitoring crop canopy temperature using a moving sprinkler system as a platform. *Applied Eng. in Agric.* 26(2): 331-341.
- O'Shaughnessy, S. A., and S. R. Evett. 2010b. Canopy temperature based system effectively schedules and controls center-pivot irrigation of cotton. *Agric. Water Mgmt.* 97(9): 1310-1316.
- O'Shaughnessy, S. A., S. R. Evett, P. D. Colaizzi, and T. A. Howell. 2012. A crop water stress index and time threshold for automatic irrigation scheduling of grain sorghum. *Agric. Water Mgmt.* 107: 122-132.
- Park, A. B., R. N. Colwell, and V. I. Myers. 1968. Resource survey by satellite: Science fiction coming true. In *USDA Yearbook of Agriculture*, 13-19. Washington, D. C.: USDA.
- Priestley, R., and R. Taylor. 1972. On the assessment of surface heat flux and evaporation using large-scale parameters. *Monthly Weather Rev.* 100(2): 81-92.
- Santanello, J. A., Jr., and M. A. Friedl. 2003. Diurnal covariation in soil heat flux and net radiation. *J. Appl. Meteorol.* 42(6): 851-862.
- Schneider, A. D., and T. A. Howell. 2000. Surface runoff due to LEPA and spray irrigation of a slowly permeable soil. *Trans ASAE* 43(5): 1089-1095.
- Todd, R. W., S. R. Evett, and T. A. Howell. 2000. The Bowen ratio-energy balance method for estimating latent heat flux of irrigated alfalfa evaluated in a semi-arid, advective environment. *Agric. Forest Meteorol.* 103(4): 335-348.
- Tolk, J. A., T. A. Howell, J. L. Steiner, and D. R. Krieg. 1995. Aerodynamic characteristics of corn as determined by energy balance techniques. *Agron. J.* 87(4): 464-473.
- Tolk, J. A., S. R. Evett, and T. A. Howell. 2006. Advection influences on evapotranspiration of alfalfa in a semiarid climate. *Agron. J.* 98(6): 1646-1654.
- Twine, T. E., W. P. Kustas, J. M. Norman, D. R. Cook, P. R. Houser, T. P. Meyers, J. H. Prueger, P. J. Starks, and M. L. Wesley. 2000. Correcting eddy-covariance flux underestimates over a grassland. *Agric. Forest Meteorol.* 103(3): 279-300.
- USDA-NASS. 2008. *Farm and Ranch Irrigation Survey, Vol. 3, Special Studies, Part 1*. Washington, D. C.: USDA National Agricultural Statistics Service. Available at: www.agcensus.usda.gov/Publications/2007/Online_Highlights/. Accessed 8 August 2011.
- USDA-NRCS. 2011. Soil Survey TX375: Potter County, Texas. Washington, D. C.: USDA Natural Resources Conservation Service. Available at: <http://websoilsurvey.nrcs.usda.gov>. Accessed 8 August 2011.
- Wanjura, D. F., and D. R. Upchurch. 1996. Time thresholds for canopy temperature-based irrigation. In *Proc. Intl. Conf. Evapotranspiration and Irrigation Scheduling*, 295-303. St. Joseph, Mich.: ASAE.